

Surface chemistry of cement pastes: a study by x-ray photoelectron spectroscopy

Maria Inês Baeta Neves,¹ Victor Oliva,¹ Béchir Mrabet,¹ Carole Connan,¹ Mohamed M. Chehimi,^{1*} Michel Delamar,¹ Simon Hutton,² Adam Roberts² and Karim Benzarti³

¹ Interfaces, Traitement, Organisation et Dynamique des Systèmes (ITODYS), Université Paris 7-Denis Diderot, associé au CNRS (UMR 7086), 1 rue Guy de la Brosse, 75005 Paris, France

² Kratos Analytical Ltd, Wharfside, Trafford Wharf Road, Manchester M17 1GP, UK

³ Laboratoire Central des Ponts & Chaussées (LCPC), 58 boulevard Lefèbvre, 75015 Paris, France

Received 8 May 2002; Revised 11 July 2002; Accepted 12 July 2002

Two cement pastes commonly used in concrete formulations were characterized by XPS before and after coating with an epoxy resin and a hardener. The XPS allowed the surface chemistry change induced by the organic coating to be monitored. In particular, the C 1s spectra were peak fitted in order to deduce the contribution of the organic materials to the total carbon content on the surface. Inspection of the N 1s peak at the cement/hardener interface indicates a certain degree of donor–acceptor interaction, where the aminated hardener plays the role of the Lewis base (donor) and the cement acts as the Lewis acid.

A relationship has been established between the dispersive contribution to the surface free energy (γ_s^d) of the cement pastes and the surface chemical composition. A substantial decrease in the surface energy (from 65 to ~ 30 mJ m⁻²) of the materials has been observed for a higher surface content in organic materials or, alternatively, for a more homogeneous organic coating even at a lower mass loading of the resin or hardener. Copyright © 2002 John Wiley & Sons, Ltd.

KEYWORDS: cement paste; epoxy resin; hardener; x-ray photoelectron spectroscopy (XPS); surface energy

INTRODUCTION

In the field of civil engineering, polymer adhesives such as epoxy resins are attracting more and more interest. They are mainly applied to the repair of concrete structures (bridges, walls) by crack injection, or by adhesive bonding of composite or steel plates in order to restore the integrity of the damaged structure.^{1,2} Adhesives also open up new possibilities for the design of bridges, because massive elements of the concrete structure could be assembled in the future by adhesive bonding. However, the mechanisms of adhesion between concrete and polymer adhesives are not well understood and thus the long-term stability of the concrete–adhesive joints is yet to be predicted. It is therefore necessary to acquire fundamental knowledge about the physicochemical interactions that occur at concrete/polymer interfaces.

The industrial preparation of cements is illustrated in Fig. 1. Basically, limestone and clay are ground and heated at 1450 °C and then quickly cooled to yield a material called

‘clinker’. Additives and fillers can be added to the clinker to obtain modified cements.

Cement pastes are obtained simply by mixing cement and water and then dried. It follows that cement pastes are mixtures of hydrates in various proportions, such as calcium silicate hydrate (CaO–SiO₂–H₂O) and calcium hydroxide (Ca(OH)₂).

Epoxy resin (e.g. diglycidyl ether of bisphenol A (DGEBA)) is one type of adhesive used in civil engineering for assembling concrete blocks. It can be crosslinked with an aminated hardener (e.g. triethylenetetramine) and the structures of these organic species are illustrated in Fig. 2.

Assembling concrete blocks or repairing damaged structures using adhesives depends strongly on the adhesion at the concrete/adhesive interface and thus on the strength of the molecular interactions between the inorganic substrates and the organic materials. Although restricted to macroscopic observations, the study of Saraswathy *et al.*³ has been devoted to the influence of the substrate surface condition and moisture content on the adhesion strength of an acrylic resin-based coating to a concrete substrate. Such a study was inserted within a more expanded work where the surface strength of a concrete substrate is influenced by the cement content, the water/cement mass ratio (W/C) and the curing time.

In a previous paper⁴ we dealt with inverse gas chromatography (IGC) of the surface energy of two cement

*Correspondence to: Mohamed M. Chehimi, Interfaces Traitement, Organisation et Dynamique des Systèmes (ITODYS), Université Paris 7-Denis Diderot, associé au CNRS, 1 rue Guy de la Brosse, 75005 Paris, France. E-mail: chehimi@paris7.jussieu.fr
Contract/grant sponsor: LCPC.
Contract/grant sponsor: Université Paris 7; Contract/grant number: 2000-C0061.

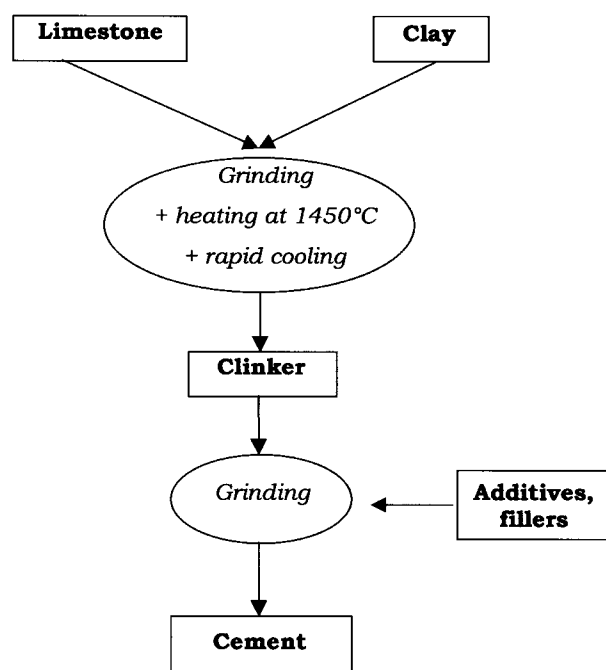
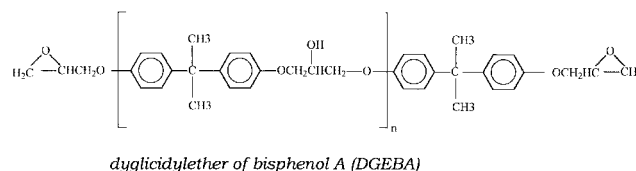


Figure 1. Industrial preparation of cements.

pastes—an ordinary Portland cement (OPC) and a blended cement (BC)—the compositions of which are displayed in Table 1. Inverse gas chromatography is a very well accepted method for assessment of the dispersive contribution to the surface energy (γ_s^d) and acid–base descriptors of electron donor–acceptor interactions. These parameters



Triethylene tetramine

Figure 2. Chemical structures of the epoxy resin and the hardener.

are of paramount importance in the study of the reversible work of adhesion. We found that the cement pastes behave as high-energy materials that are amphoteric with a predominant basicity. Coating with an epoxy resin or a hardener resulted in a substantial decrease of the surface energy as a function of the mass loading of the organic materials. The two cements behave in a similar manner when bare or coated with the epoxy resin. Interestingly, it was found that the hardener decreases more significantly the surface energy of the OPC cement than the resin for the same mass loading (1 wt.%), perhaps indicating a better wetting.

Changes in the surface thermodynamics of the cement pastes were related to the crude initial mass loading of resin or hardener and to the $(\text{C} + \text{N})/(\text{Ca} + \text{Si} + \text{O})$ atomic ratio. The latter was used as a rough measure of organic/inorganic material content.

Table 1. General applications and chemical properties of ordinary portland cement (OPC) and blended cement (BC) pastes

	OPC ^a	BC ^b
Applications	<ul style="list-style-type: none"> • Offshore applications • Reinforced concrete, high-performance concrete • Applications at ambient or low temperature • Civil structures where high performances are required 	<ul style="list-style-type: none"> • Applications where high initial performances are needed • Underground works in non-aggressive media • Masonry, ground stabilization
Composition	Clinker ~97%	65% < clinker < 79% 21% < carbonate fillers + gypsum < 35%
Mineral composition ^c		
C ₃ S	57.63%	37.11%
C ₂ S	17.84%	18.45%
C ₃ A	2.22%	8.22%
C ₄ AF	12.64%	7.59%
Carbonate content	2.00%	22.39%
Gypsum	6.15%	6.24%

^a Industrial product CPA CEM I 52.5 PMES from Lafarge, Le Havre, France.

^b Industrial product CPJ CEM II B 32.5 R, from Lafarge, Frangey, France.

^c Cement chemists' notation is used throughout: C = CaO; S = SiO₂; A = Al₂O₃; F = Fe₂O₃; S = SO₃.

Of relevance to this ongoing research programme, Chehimi and co-workers have related the surface energy to the surface chemistry changes of conducting polypyrrole (a high-energy polymer) powders as a result of the adsorption of homopolymers⁵ and polymer blends.⁶ Such relationships allowed the mechanisms by which adsorbates interact and wet the conducting polymer surfaces to be understood.

Back in the early 1990s, Kokodan *et al.*,⁷ in their XPS and contact angle measurement studies of thermoplastic fibre composites, related the polar component γ_s^p of the surface free energy of the composites to the various C 1s components located at high binding energy and corresponding to polar functional groups such as C–O, C=O, N–C=O bonds, etc. In this study, the C 1s peaks from the composites were fitted in order to determine the relative concentration of oxygen-containing species and to deduce a weighted dipole moment for each composite using the dipole moments of the polar chemical bonds. Kodokian *et al.* established a relationship between the weighted dipole moment of the composites and their corresponding γ_s^p values.

The aim of this paper is a detailed XPS study to characterize the surface chemical composition of two cement pastes before and after coating with an epoxy resin or triethylenetetramine (an aminated hardener). The emphasis is mostly on the surface composition as well as the fine structure of the C 1s peaks and their organic and inorganic material contributions, the latter essentially being due to carbonates. The surface energy/surface chemistry correlation for the cement pastes is revised. It focuses now on the interfacial chemistry of the cement paste/organic coating system rather than on the mass loading of the resin or hardener.

EXPERIMENTAL

Materials

Table 1 reports the main applications and mineral composition of the two cement pastes studied. Although OPC is almost a pure clinker, BC is 71% clinker and 23% chalky filler. These cement pastes have been prepared with a water/cement proportion of 0.5 wt.%. The resin used was DGEBA (Araldite resin CY230, Ciba Performance Polymers, 92506 Rueil Malmaison, France) and the hardener was triethylenetetramine (HY956, Ciba Performance Polymers, 92506 Rueil Malmaison, France).

For the purpose of coating the materials, the well-known method of Al-Saïgh and Munk was chosen.⁸ The exact mass of resin (or hardener) is dissolved in 50 ml of acetone (Prolabo, Fontenay Sous Bois, France), then the material to be coated is placed on a clock glass or a Pétri dish and is slowly impregnated with drops of the solution of acetone and resin (or hardener). The liquid must not touch the glassy vessel walls, otherwise there would be a great loss of resin (or hardener). When the solvent has evaporated, the material is mixed and the whole process is repeated. This method is time consuming but is very accurate (associated error is typically $\leq 1\%$) and does not require further checking by thermal gravimetric analysis or ashing.⁹ The specimens are denoted OPC-R, OPC-H, BC-R and BC-H for resin (R)-coated and hardener(H)-coated OPC and BC cement pastes.

These abbreviations are followed by the mass loading of organic coating. For example, OPC coated with 1 wt.% resin is denoted OPC-R1%.

Scanning electron microscopy

Scanning electron micrographs were obtained with a Philips XL30 instrument equipped with EDAX DX4 (Philips Optique Electronique, Limeil-Brévannes Cedex, France). The equipment is completely controlled from a computer workstation. The XL series instruments are controlled by a personal computer running Microsoft Windows NT. The filament is a zirconated tungsten and the accelerating voltage was set at 5 kV.

X-ray photoelectron spectroscopy

A VG Scientific Escalab MK 1 spectrometer (East Grinstead, UK) equipped with a twin anode was used. A polychromatic Al K α x-ray source (1486.6 eV) was selected and operated at a power of 200 W (10 kV with an emission current of 20 mA). The pass energy was set at 50 eV. The take-off angle was 0° relative to the surface normal. The pressure in the analysis chamber was $\sim 10^{-8}$ mbar. The data were collected with Pisce software (Dayta Systems, Bristol, UK). The step size was 1 eV for the survey scan and 0.1 eV for the narrow scan.

Data processing was achieved with Winspec software, kindly supplied by the Laboratoire Interdisciplinaire de Spectroscopie Electronique (LISE, Namur, Belgium). The spectra were corrected for static charging by setting the C 1s peak maximum at 285 eV. The surface composition was determined using experimental sensitivity factors. The fractional concentration of a particular element A (% A) was computed using

$$\%A = \frac{(I_A/S_A)}{\sum (I_n/S_n)} \times 100$$

where I_n and S_n are the integrated peak areas and the sensitivity factors, respectively. The sensitivity factors were determined with reference organic and inorganic compounds of well-defined stoichiometries.

The ultimate spectral resolution of C 1s peaks was achieved using a Kratos Axis Ultra photoelectron spectrometer (Manchester, UK). This instrument is equipped with a monochromated Al K α x-ray source operating at 300 W and a fully automatic coaxial low-energy electron source that ensures a uniform charge compensation even for highly topographic powdery insulating materials. The pass energy was set at 10 eV. The take-off angle was 0° relative to the surface normal. Spectra were charge referenced to the hydrocarbon component at 285 eV binding energy. Surface compositions were determined using the manufacturer's sensitivity factors.

RESULTS AND DISCUSSION

Scanning electron micrographs of cement paste surfaces

Figure 3 presents scanning electron micrographs of an OPC before coating, OPC-H1%, OPC-R1% and OPC-R5%. The surface of the cement paste coated with the epoxy resin of mass

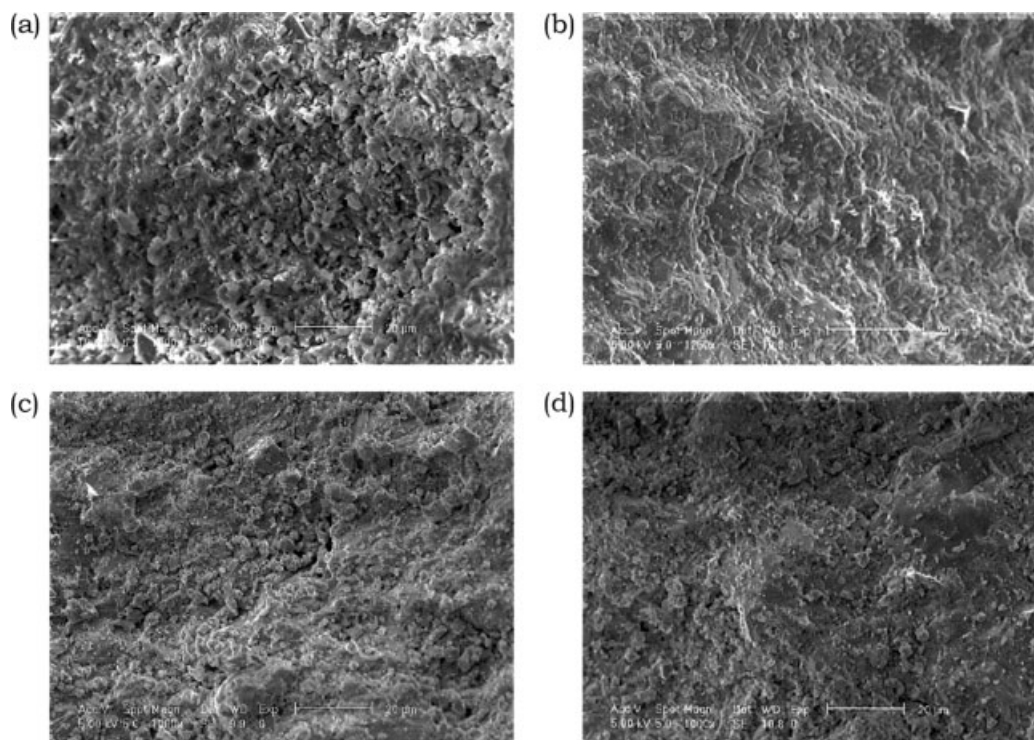


Figure 3. Scanning electron micrographs of: (a) an OPC paste before coating; (b) OPC-H1%; (c) OPC-R1%; (d) OPC-R5%.

loading 5% exhibits very smooth areas due to the organic coating. In contrast, the difference between OPC and OPC coated with either 1 wt.% hardener or resin is only subtle. This difference will be much more exacerbated by the XPS.

Surface analysis by XPS

Survey spectra

Figure 4 shows the XPS survey spectra of a BC specimen before and after coating with the epoxy resin and the hardener. Survey scans acquired using a monochromated x-ray source correspond to the BC paste before and after coating with the hardener (Figs 4(c) and 4(d)). Several elements are readily detected (Al, Mg, Na, etc.) in addition to the main ones of silicon, calcium, oxygen and carbon, the corresponding photopeaks of which are Si 2p, Ca 2p, O 1s and C 1s centred at 103 (Si 2p), 347 (Ca 2p), 531 (O 1s) and 285 eV (C 1s), respectively. The hardener exhibits an additional N 1s peak centred at 400 eV (Fig. 4(d)).

The survey spectra acquired with the Escalab Mk 1 equipped with a polychromatic twin anode are also very informative from a qualitative point of view, despite their lower signal-to-noise ratios. Indeed, one can note the increase in the post-peak slope in the 550–950 eV binding energy range for the BC paste coated with 5 wt.% epoxy resin (BC-R5%) in comparison with the uncoated BC substrate (Figs 4(a) and 4(b)). As discussed in detail by Castle in one of his recent papers,¹⁰ such a positive increase in the background is due to the attenuation in intensity of the photopeaks arising from the cement substrate, induced by the resin overlayer.

Surface elemental composition

Table 2 reports the surface elemental composition (in at.%) for the untreated and coated cement pastes. Here we have

considered only the most important elements, i.e. carbon, nitrogen, oxygen, calcium and silicon. The elements Na, Mg, Cl, S and K were omitted because they make only a minor contribution to the surface composition in comparison with the essential elements constituting the cement pastes (Ca, Si and O). The carbon content (%C) invariably increases at the surface of OPC and BC following organic coating with either epoxy or hardener. In the case of coating with 5 wt.% epoxy, the %C is twice as high as for uncoated OPC and 50% higher than for uncoated BC. There is also a slight decrease of the oxygen content after coating due to attenuation of calcium silicates and other oxides. The decrease in the calcium content is very small but measurable, whereas the silicon content has no clear variation with organic coating, especially in the case of BC. These observations are consistent with the shape of the survey spectrum displayed in Fig. 4(b).

Carbon 1s

Figure 5 displays peak-fitted C 1s signals from BC, BC-R1%, BC-R5% and BC-H1%. All the C 1s spectra exhibit complex structures, with the two apparent main peaks centred at 285 and ~290 eV due to aliphatic (C–C/C–H), aromatic (C=C) carbon and carbonaceous species (C–O, C=O) on the one hand, and carbonates on the other. We define these two main peaks as C1s₂₈₅ and C1s₂₉₀. In addition, one can also note the K 2p_{3/2}–K 2p_{1/2} doublet at higher binding energy (293–293.5 and 295.8–296.3 eV, respectively). The spectra have shapes similar to those obtained for CaO and MgO freshly exposed to CO₂.¹¹ In our case the major contribution of carbonates is due to calcium carbonates.

For the untreated cements, the first complex C1s₂₈₅ peak is due to adventitious contamination. It is noteworthy that the C1s₂₈₅/C1s₂₉₀ intensity ratio increases with organic material

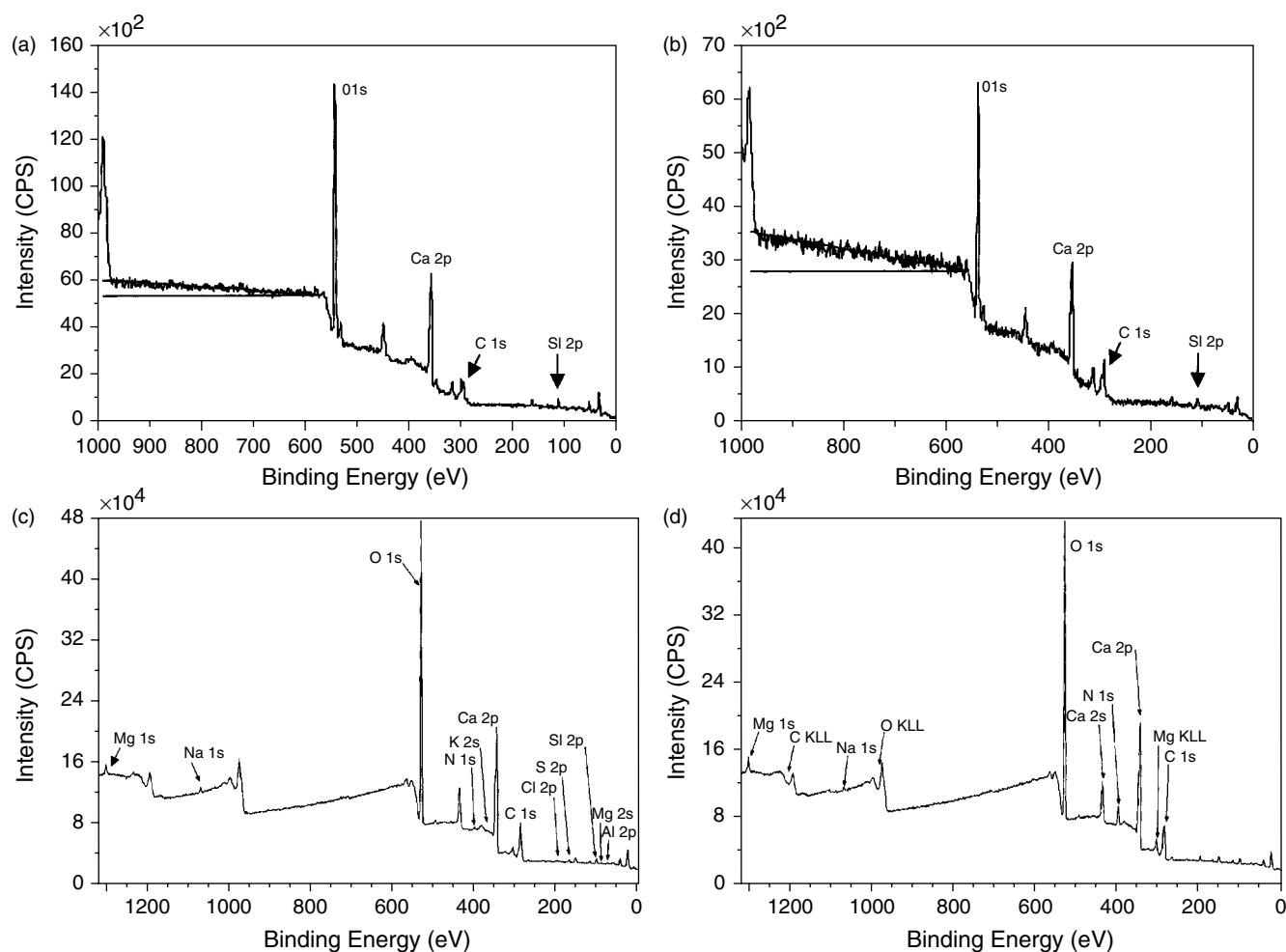


Figure 4. The XPS survey spectra of a BC specimen before (a, c) and after coating with the epoxy resin (b) and the hardener (d). Spectra (a) and (b) were obtained with a polychromatic x-ray source, and spectra (c) and (d) with a monochromated x-ray source.

Table 2. Surface composition (at.%) of uncoated and coated cement pastes^a

Cement paste	C	O	N	Si	Ca
BC	19.3	59.8		3.73	17.2
BC + R1%	22.4	55.8		2.87	18.9
BC + R5%	27.6	52.7		4.02	15.7
BC + H1%	22.2	54.7	3.17	3.60	16.3
OPC	13.6	60.5		6.32	19.6
OPC + R1%	29.8	52.1		1.98	16.1
OPC + R5%	25.9	52.8		4.50	16.8
OPC + H1%	25.1	50.0	5.14	4.03	15.7

^a BC = blended cement; OPC = ordinary Portland cement; R1% = epoxy resin 1%; R5% = epoxy resin 5%; H1% = hardener 1%.

loading until the first composite C1s₂₈₅ peak becomes the main one.

In the case of the uncoated and the coated cement pastes, the C 1s spectra were fitted with four components. The first four components are centred at 285, 286.1–286.8, 287.5–288.8 and 289.3–290.7 eV, which we assign to CC/CH, C–O, C=O and CO₃²⁻, respectively.

In the case of the hardener-coated cement pastes, the C–N C 1s component actually partly fills the gap between the two maxima centred at 285 and 289.5 eV because it contributes to the C 1s peak at a binding energy of ~286.0 eV.

It is interesting to note that the C1s₂₈₅ peak from BC-H1% is fairly wide in comparison with BC, BC-R1% and BC-R5%. This is due to the fact that all carbon atoms in the hardener are involved in C–N bonds, of which the corresponding C 1s component is expected at ~286 eV. This markedly differs for the BC-R1% and BC-R5% specimens because in the epoxy resin there are two major types of carbons: aromatic C=C and aliphatic CC/CH bonds; and C–O bonds. Taking into account the chemical structure of the epoxy resin shown in Fig. 2, one can split the whole carbon atoms into two types: 39 C=C/C–C/C–H bond carbon types, and 18 C–O bond carbon types. The corresponding C 1s components of these types of carbons are expected at 285 and 286–286.5 eV, respectively, with a theoretical intensity ratio of 18/39 = 0.46. For the uncoated BC specimen the experimental C–O/(C–C/C–H) intensity ratio is 0.27, and for the BC-R5% specimen it is 0.33. Obviously, one cannot reach the maximum value expected for the epoxy resin because the substrate is still detected through the organic overlayer.

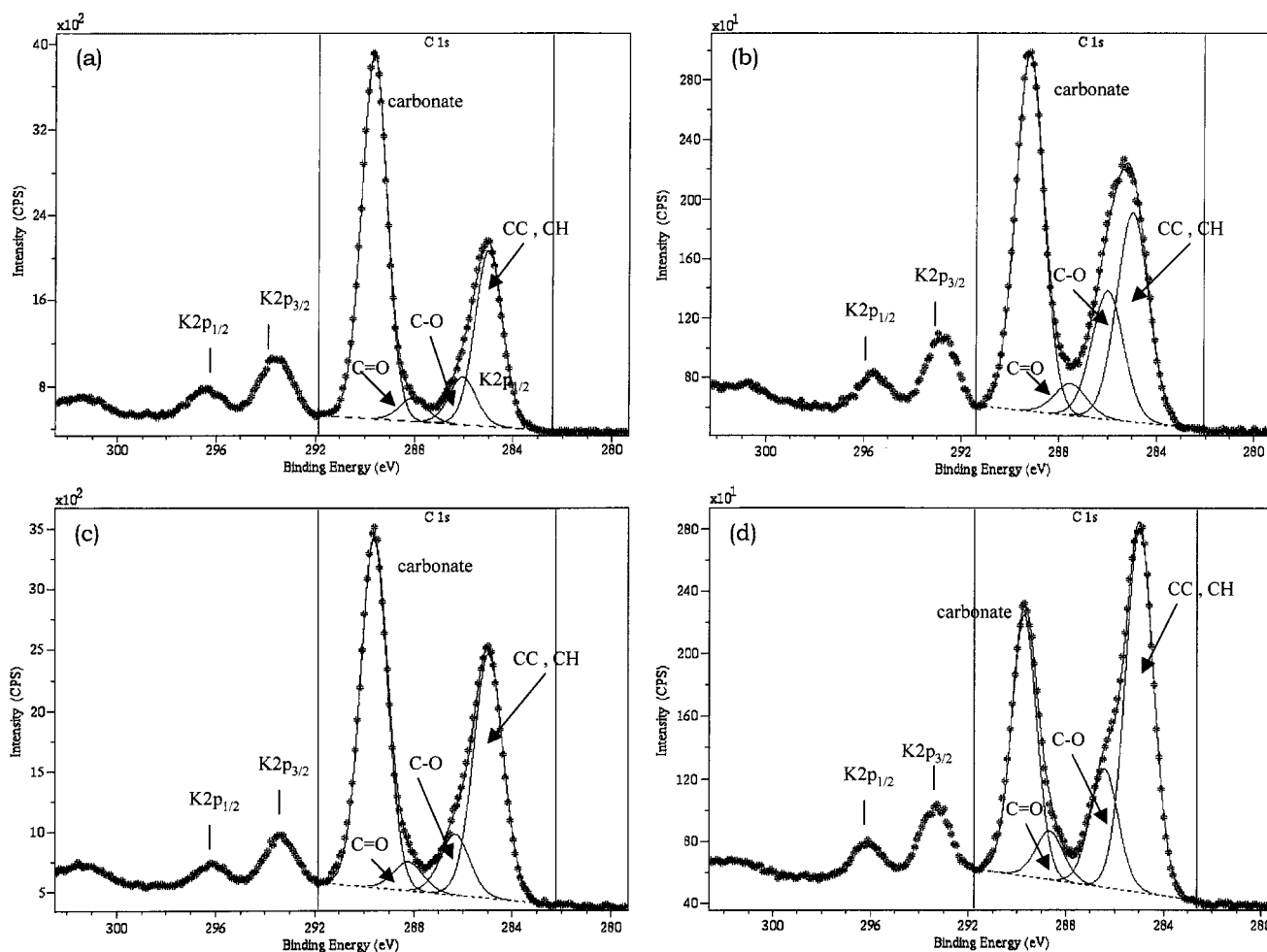


Figure 5. Peak-fitted C 1s signals from uncoated BC, BC-R1%, BC-R5% and BC-H1%.

In the case of the BC-H1% specimen and as mentioned above, the only C 1s component due to the hardener is due to C–N bonds and thus is expected at a binding energy close to 286 eV. The hardener contributes thus to the second C 1s component only, which leads to the highest intensity ratio (0.61) if one considers the second C 1s component (in which C–N and C–O bonds are lumped together) centred at 286 eV and the main one due to CC/CH bonds centred at 285 eV. This is the reason why the C1s₂₈₅ peak from BC-H1% looks much wider than those of BC, BC-R1% and BC-R5%. Lumping the C–O and C–N components for the BC-H1% specimen resulted in C–C/C–H and C–O/C–N C 1s components having a full width at half-maximum (FWHM) of 1.51 eV, whereas for BC, BC-R1% and BC-R5% the component centred at 286 eV has an FWHM of 1.29–1.39 eV.

Taking into account the C–N bonds in the hardener, one can obtain the C 1s peak fitting shown in Fig. 6 for BC-H1%, with C 1s components in the first complex peak having FWHM values in the 1.02–1.38 eV range.

Table 3 reports C 1s peak fitting parameters for BC and OPC before and after coatings, and one can see the much lower contribution of the carbonate species at the surface of the coated OPC specimens. It is worth noting that for the coated BC the C1s₂₉₀ reaches a contribution of 40–48%, which levels off at 27% for the coated OPC (OPC-R1%), perhaps

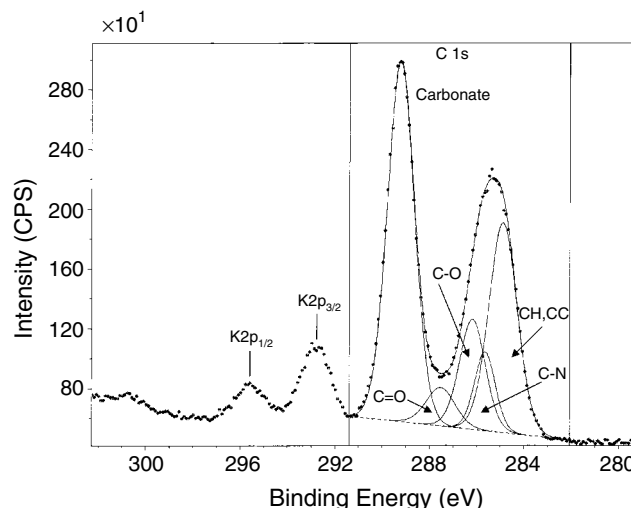


Figure 6. Carbon 1s peak fitting for BC-H1%, taking into account the C–N bonds in the hardener.

indicating a better wetting of OPC by the organic materials than BC.

Nitrogen 1s

The high-resolution N 1s spectrum of BC-H1% (and similarly in the case of OPC-H1%) was fitted with two components

Table 3. Carbon 1s peak fitting and relative peak area ratios (%) for uncoated and coated cement pastes

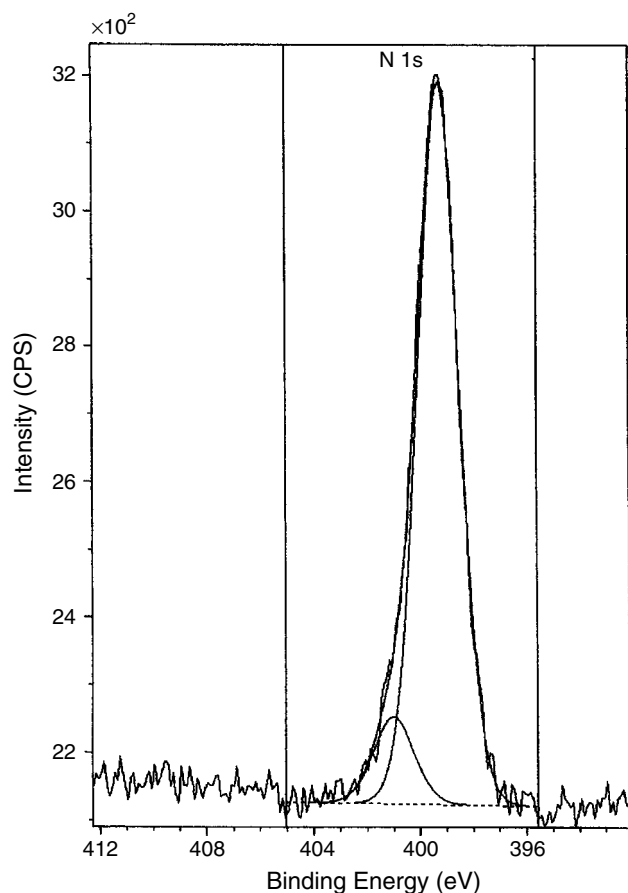
		C=C/CC/CH	C-N	C-C-OH/C-O-C	C=O/O-C=O	CO ₃ ²⁻
BE range (eV)		285	286–286.2	286.1–286.8	287.5–288.8	289.3–290.7
BC	Escalab	28.8		16.2	12.4	34.9
	Kratos	30.5		8.24	4.02	57.3
BC-H1%	Escalab	29.6	17.7	10.2	7.47	30.4
	Kratos					
BC-R1%	Escalab	29.7		17.3	10.8	40.2
	Kratos	37.9		9.47	4.48	48.2
BC-R5%	Escalab	44.3		19.9	13.8	18.0
	Kratos	47.5		15.6	6.38	30.6
OPC		36.8		13.5	9.29	38.0
OPC-H1%		25.5	18.7	14.2	16.6	23.1
OPC-R1%		31.7		26.9	12.5	26.9
OPC-R5%		44.6		24.1	8.66	20.9

BC = blended cement; OPC = ordinary Portland cement; R1% = epoxy resin 1%; R5% = epoxy resin 5%; H1% = hardener 1%.

centred at 399.3 and 401.0 eV, respectively (Fig. 7). The minor high-binding-energy component is likely to be due to hydrogen bonds at the cement paste/hardener interface. Quaternized nitrogen from the hardener is unlikely because the N 1s binding energy for such species is significantly higher than 401 eV and, moreover, the cement paste aqueous suspensions yield pH 12 due to their Brönsted basicity.

Chemical shifts similar to that shown in Fig. 7 have been reported in the literature for molecular species such

as pyridine adsorbed onto zeolites,¹² chloroform and other molecular probes adsorbed on untreated^{13,14} and plasma-treated polymer surfaces^{14–16} and alcohols/diamines on metal surfaces.¹⁷ In the case of thin polymethyl methacrylate (PMMA) overlayers coated on inorganic substrates, chemical shifts due to polymer–metal oxide interactions were observed at the surface of silica¹⁸ and alumina.¹⁹ In the present case, the donating ability of the hardener's nitrogen atoms to the cement paste surface is in line with the amphoteric behaviour of the inorganic substrate and particularly its Lewis acidity as determined by IGC.⁴

**Figure 7.** High-resolution N 1s spectrum of BC-H1%.

Relationship between the surface chemistry and the surface energy

For the purpose of this paper we related the surface energy to the surface chemistry of the materials. The γ_s^d values determined at 35 °C by IGC were plotted versus the $(C_{org} + N)/(Ca + Si + O)$ atomic ratio as determined by XPS, where C_{org} stands for the organic material contribution to the total carbon content at the surface. This means that the carbonate C 1s component has been extracted from the C1s peak fitting. The atomic ratio defined above was chosen as a surface chemical descriptor for the quantitative measure of organic/inorganic material content. As far as the surface thermodynamic properties are concerned, we have chosen γ_s^d as the descriptor parameter for the specimens. This choice was driven by the fact that dispersive properties are ubiquitous so that all types of materials and consequently chemical bonds contribute to the strength of dispersive interactions. This is, of course, not the case for the more specific acid–base or dipolar interactions. In a similar way, Abel *et al.* have related the γ_s^d values of polypyrrole powders (high-energy conducting polymers) to their surface composition before and after coating with PMMA⁵ and PMMA–PVC blends.⁶

Figure 8 shows a relationship between γ_s^d values and the surface chemistry descriptor. It is worth noting the distinct decreasing trend of the surface energy with the concentration of elements characteristic of organic materials loaded on the cement pastes.

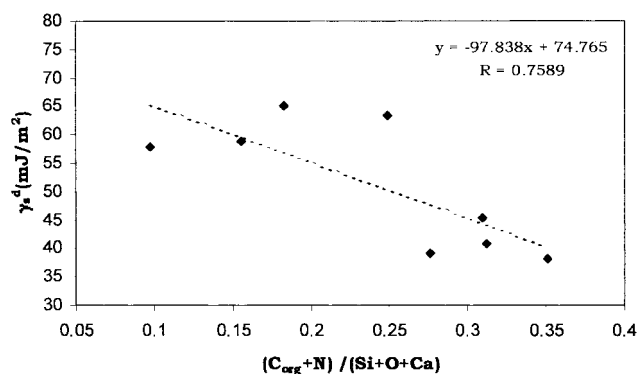


Figure 8. Relationship between γ_s^d values and the surface chemistry descriptor for uncoated and coated OPC and BC pastes.

This approach is clearly much more precise and elegant than the relationship between the surface energy and the mass loading of the organic materials because the latter parameter reflects the preparation of the materials but in no way the actual surface chemistry that accounts for the adsorption and wetting of the inorganic substrate by the organic epoxy resin or the hardener.

CONCLUSION

Two cement pastes (OPC and BC) were characterized by XPS before and after coating with epoxy resin and triethylene tetramine (hardener). The specimens were analysed in a powdery form that was amenable to both XPS and surface energy studies by IGC. The change in the surface composition of the cements was monitored by XPS as a function of the organic material loading. Inspection of the C 1s peaks obtained at an ultimate spectral resolution using a monochromated Al K α x-ray source permitted the organic moieties at the surface of cements and the carbonate species from the substrates to be distinguished unambiguously. The high-resolution N 1s peak fitted with two components suggests an interfacial-specific cement–hardener interaction where the minor high-binding-energy N 1s component is due to the electron-donating ability of the nitrogen atoms towards the acidic surface sites of the cements. This is in line with the amphoteric behaviour of cement pastes as judged from a previous IGC study.⁴ Using equipment with an ultimate spectral resolution also permitted deeper insight into the interfacial chemistry at the cement/organic coating interface.

The surface chemical composition determined by XPS has been correlated with the dispersive contribution to the

surface energy (γ_s^d) of the cement pastes. Interestingly, it was found that the hardener decreases more significantly the surface energy of OPC cement than the resin, indicating perhaps a better wetting. This is in line with a much stronger attenuation of the Si 2p, Ca 2p and carbonate C 1s XPS peaks from OPC.

This combined surface chemistry–surface energy study of cement pastes is of technological importance because it is related to the adhesion aspects of concrete assemblies using high-performance adhesives.

Acknowledgements

The authors would like to thank LCPC and Université Paris 7 for financial support (research project 2000-C0061) and T. Berthelot for technical assistance with the SEM equipment.

REFERENCES

- Karhari VM, Zhao L. *Computer Methods Appl. Mech. Eng.* 2000; **185**: 433.
- Theillout J-N. In *Proc. Symp. RILEM ISAP 86*. Chapman & Hall: New York, 1986; 601–621.
- Saraswathy V, Rengaswamy NS. *J. Adhes. Sci. Technol.* 1998; **12**: 681.
- Oliva V, Mrabet B, Baeta Neves MI, Chehimi MM, Benzarti K. *J. Chromatogr. A*, in press.
- Chehimi MM, Abel M-L, Sahraoui Z. *J. Adhes. Sci. Technol.* 1996; **10**: 287.
- Abel M-L, Chehimi MM, Fricker F, Delamar M, Brown AM, Watts JF. *J. Chromatogr. A*, in press.
- Kinloch AJ, Kodokian GKA, Watts JF. *Philos. Trans. R. Soc. London A*. 1992; **338**: 83.
- Al-Saigh Z, Munk P. *Macromolecules* 1984; **17**: 803.
- Demathieu C. *PhD Thesis*. Université Paris 7, 1998.
- Castle JE. *Surf. Interface Anal.* 2002; **33**: 196.
- Alarcón N, García X, Centeno M, Ruiz P, Gordon A. *Surf. Interface Anal.* 2001; **31**: 1031.
- Huang M, Adnot A, Kaliaguine S. *J. Catal.* 1992; **137**: 322.
- Chehimi MM, Watts JF, Eldred WK, Fraoua K, Simon M. *J. Mater. Chem.* 1994; **4**: 305.
- Chehimi MM, Delamar M, Kurdi J, Arefi-Khonsari F, Lavaste V, Watts JF. In *Acid–Base Interactions: Relevance to Adhesion Science and Technology*, vol. 2., Mittal KL (ed.). VSP: Utrecht, The Netherlands, 2000; 275–298.
- Shahidzadeh N, Chehimi MM, Arefi-Khonsari F, Foulon-Belkacemi N, Amouroux J, Delamar M. *Colloids Surf. A* 1995; **105**: 277.
- Shahidzadeh N, Chehimi MM, Arefi-Khonsari F, Amouroux J, Delamar M. *Plasmas Polym.* 1996; **1**: 27.
- Barthes-Labrousse M-G, Joud J-C. In *Acid–Base Interactions: Relevance to Adhesion Science and Technology*, Vol. 2., Mittal KL (ed.). VSP: Utrecht, The Netherlands, 2000; 453–463.
- Beamson G, Bunn A, Briggs D. *Surf. Interface Anal.* 1991; **17**: 105.
- Leadley SR, Watts JF. *J. Adhes.* 1997; **60**: 175.